

NORTHEASTERN UNIVERSITY

UNDERGRADUATE THESIS

**An Improved Method for Real-Time
Ratiometric Quantitative Fluorescent
Microscopy in the Pharynx of *C. elegans***

Author:
Sean Johnsen

Supervisor:
Dr. Javier Apfeld

*A thesis submitted in fulfillment of the requirements
for the degree of Bachelor of Science*

in the

Department of Biology

April 17, 2019

“...the grandest discoveries of science have been but the rewards of accurate measurement and patient long-continued labour in the minute sifting of numerical results.”

Lord Kelvin

NORTHEASTERN UNIVERSITY

Abstract

Faculty Name
Department of Biology

Bachelor of Science

**An Improved Method for Real-Time Ratiometric Quantitative Fluorescent
Microscopy in the Pharynx of *C. elegans***

by Sean Johnsen

The abstract goes here...

Acknowledgements

The acknowledgments and the people to thank go here. . .

Contents

Abstract	ii
Acknowledgements	iii
1 Introduction	1
1.1 Fluorescent biomarkers enable real-time quantification of cytosolic protein oxidation	1
1.2 Limitations of current pipeline	2
1.2.1 Inter-frame movement results in measurement error	2
1.2.2 Segmentation and centerline estimation sometimes require manual input	3
1.3 Aims	4
2 Methods	5
2.1 Edge information helps to differentiate the pharynx from the intestine	5
2.2 Flexible measurement boundaries allow for anterior-posterior movement	6
2.3 Midlines	6
2.3.1 A transmitted light image helps to anchor the midlines	6
2.3.2 Dorsal-ventral movement of the tip is a problem	7
2.4 Channel Registration picks up the slack	7
3 Results	8
3.1 Definition of Error	8
3.2 Collection of test data	8
3.3 A Partially Synthetic Dataset Increases Statistical Power	8
3.4 Reductions in Manual Intervention	8
3.5 Channel-Specific Masks and Midlines Reduce Error	8
4 Discussion	10
4.1 Future Directions	10

List of Figures

1.1	Ratios of images to redox state	2
1.2	Pharyngeal contractions lead to boundary issues	2
1.3	Dorsal ventral movement of the tip of a pharynx	3
1.4	Dorsal ventral movement of the tip of a pharynx	3
1.5	The goal of segmentation	4
1.6	The problem with static thresholding	4
2.1	Overview of the improved segmentation algorithm	5
2.2	Overview of the improved segmentation algorithm	6
2.3	Previous centerline estimation algorithm	7
3.1	Average intensity over time in technical replicates	9
3.2	Error by strategy in the natural data set	9
3.3	Error by strategy in the synthetic data set	9

Chapter 1

Introduction

Oxidation and reduction (redox) reactions play a vital role in biology. These reactions are characterized by a flow of electrons between chemical species. The species gaining electrons is said to have been oxidized, while the species losing electrons is said to have been reduced. Redox reactions are involved in many vital processes such as cellular respiration, .

other processes

Many chemical species in the cell may exist in either an oxidized or reduced form. These *redox couples* play central roles in a variety of cellular processes. The NAD^+/NADH couple, for example, shuttles high energy electrons wrought from the oxidation of sugars in the citric acid cycle to the proton pumps in the electron transport chain. The healthy cell actively maintains a steady-state disequilibrium of these redox couples. The overall state of this network of redox couples is called the *redox state*. The impaired ability of the cell to regulate its redox state is termed *oxidative stress* and is associated with a number of diseases such as cancer, various neurological disorders, and aging. Quantifying the redox state in live cells allows a deeper understanding of the regulatory mechanisms that mediate these processes.

1.1 Fluorescent biomarkers enable real-time quantification of cytosolic protein oxidation

In a previous paper, our lab demonstrated the use of the redox-sensitive fluorescent protein roGFP to quantify the cytosolic redox state in the pharyngeal muscle of *C. elegans* in real-time. The use of these biomarkers is leading to quantitative and mathematical models of the genetics and dynamics of intracellular and organismal-level redox signaling.

The methodology relies on the dual emission spectra of the oxidized and reduced form of roGFP. By taking the ratio of emission intensity when excited at different wavelengths, we can use the Nernst equation to estimate the cellular redox state.

The quantification requires two images be taken of each pharynx — one at 410nm and another at 470nm. By dividing the brightness of the images pixel-by-pixel we can estimate the redox state at each position in two dimensions (Figure 1.1).

replace fig this with the 410nm / 470nm => E

Due to the cellular architecture of the pharynx, almost all of the variation in redox state follows the posterior-anterior axis. Thus, we can model the pharynx 1-dimensionally as the redox state along its posterior-anterior axis without losing significant information. Computationally, this is achieved by (1) estimating the centerline of the pharynx then (2) measuring the intensity of the images under this estimated centerline.

As will be discussed, a fundamental limitation of this analysis arises when the animal moves in the time between capturing the first and second frame in the pair

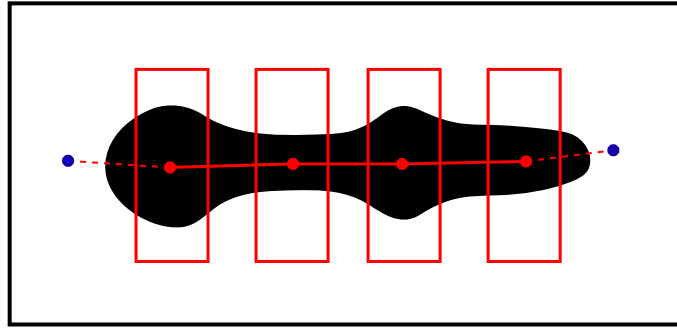


FIGURE 1.1

of images required for each animal. The aim of this thesis project was to improve the methods by which these centerline measurements were gathered and analyzed so as to reduce experimenter input and minimize errors introduced by this inter-frame movement.

1.2 Limitations of current pipeline

1.2.1 Inter-frame movement results in measurement error

The pharynx is the feeding muscle of the animal. It contracts along its anterior-posterior axis, functioning as a pump to bring in food. Animals are paralyzed prior to imaging with a 1mM solution of the actyl choline agonist levamisole. Even so, the pharyngeal muscle occasionally contracts.

This contraction poses a problem for analysis. Ordinarily, dividing intensities pixel-by-pixel is appropriate because the mapping between image space and physical space remains consistent between pairs of images. If the animal moves, however, a new mapping must be constructed for each image. To understand why, consider Figure 1.2.

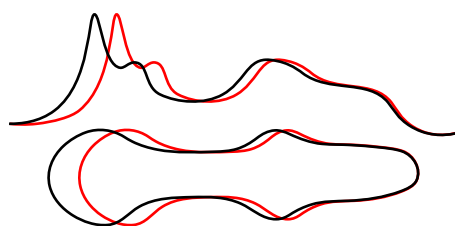


FIGURE 1.2: A cartoon shows how pharyngeal contractions lead to measurement boundary issues.

On the bottom we see the outline of the pharynx in each frame. The pharynx has contracted in one frame (red) and is elongated in the other (black). When the intensities along the posterior-anterior axis are plotted above, it is clear that the contraction has lead to unwanted compression of the intensity profile.

Another common mode of interframe movement is represented similarly in Figure 3.3. This is movement of the tip of the pharynx dorsal-ventrally. Dorsal-ventral tip movements result in a loss of information about the tip in one frame, as depicted in red.

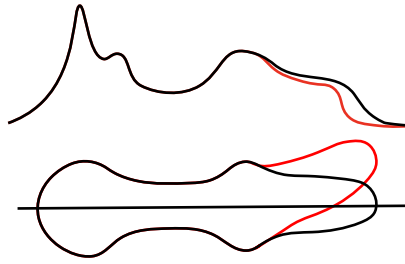


FIGURE 1.3: A cartoon shows dorsal ventral movement in the tip of the pharynx and the resultant intensity profiles measuring under the single centerline.

The current method for dealing with these problems is to visually screen the ratio images for images with a highly textured appearance, as shown in figure 1.4. These animals are then excluded from analysis. This visual screening is a time-intensive process, requires training, and is subject to experimenter error and bias.

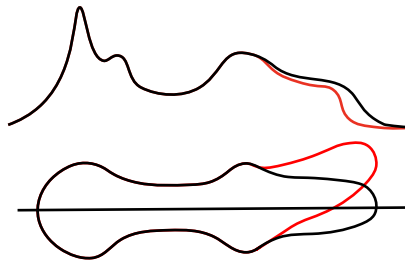


FIGURE 1.4: A cartoon shows dorsal ventral movement in the tip of the pharynx and the resultant intensity profiles measuring under the single centerline.

1.2.2 Segmentation and centerline estimation sometimes require manual input

As noted, the visual screen for inter-frame movement is a manual step. Two other processes in the current pipeline also require manual supervision. The first is segmentation. Segmentation is the process by which pixels corresponding to objects in an image are given salient labels. In our case, the task is to separate the pharynx from everything else (Figure 1.5).

Because the transgenic animals express roGFP with pharynx-specific promoters, the task is usually straightforward. However, the intestine of *C. elegans* autofluoresces in response to the wavelengths of light that we use. This poses a problem for the static thresholding algorithm currently used to segment the pharynx. This algorithm assigns any value greater than a threshold the value 1 and those below the threshold 0. Static thresholds works well when the distribution of brightness is different for each class of object in the image, but this is not the case when the intestine autofluoresces resulting in ill-formed segmentation masks (Figure 1.6).

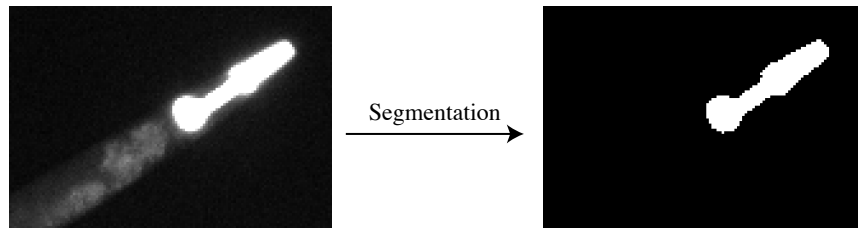


FIGURE 1.5: The goal of segmentation. On the left, the original image showing fluorescence of roGFP in the pharynx and autofluorescence in the gut. On the right, a binary image consisting of value 1 in the pixels with a pharynx and value 0 elsewhere.

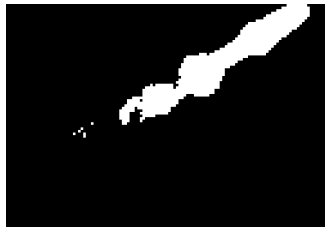


FIGURE 1.6: The problem with static thresholding. This image must be manually corrected.

1.3 Aims

This thesis aims to address the limitations of the current analysis pipeline described in 1.2.1 and 1.2.2. To achieve this, a new pipeline was written in MATLAB to process and analyze these images end-to-end with little to no necessary manual input. The improved pipeline decreases the time required to analyze this data, standardizes the analysis, reduces human error, and mitigates movement-induced error.

Chapter 2

Methods

2.1 Edge information helps to differentiate the pharynx from the intestine

As described in 1.2.2, intestinal autofluorescence causes the static thresholding algorithm to perform insufficiently in separating the pharynx from the rest of the animal and the background. Histogram-based threshold detection such as Otsu's method also perform poorly when the histograms are not bimodal, as is the case with bright intestinal autofluorescence.

To address these issues, a new segmentation algorithm was developed. This algorithm exploits *edges*, sharp changes in brightness which are information-rich regions in images. The Sobel operator creates an image emphasizing edges by discretely differentiating the image in the vertical and horizontal directions (Figure 2.1). By thresholding the resultant image, using morphological operations to remove noise, and selecting the largest region, we isolate the pharynx from gut autofluorescence.

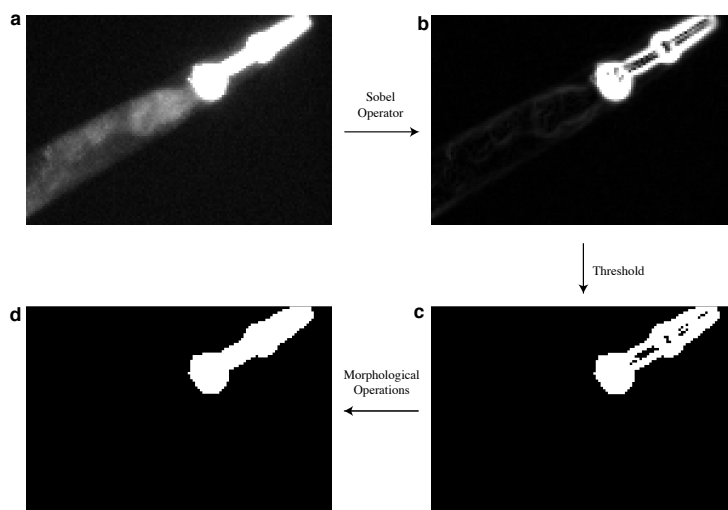


FIGURE 2.1: An overview of the improved segmentation algorithm. **a** The original image, displaying fluorescence of roGFP in the pharynx and the autofluorescence of the gut. **b** The resultant image after application of the sobel operator. **c** The resultant binary image after thresholding the edge-emphasized image. **d** The final segmented binary image, after performing morphological cleaning operations.

For reasons described in 2.3.1, an image taken with transmitted light must also

be segmented. Even though the distribution of intensities in transmitted light images are very different from fluorescence images, this edge-based segmentation algorithm still performs robustly (Figure 2.2). This highlights another benefit of the improved method: image brightness independence. If one particular genotype fluoresces dimly, an edge-based segmentation method still performs well, while the static thresholding method requires the manual change of the threshold parameter.

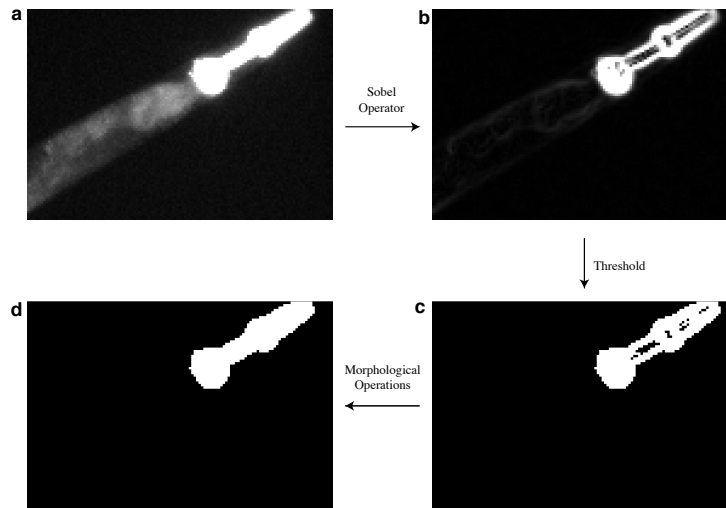


FIGURE 2.2: This should be an image of transmitted light before/after segmentation.

2.2 Flexible measurement boundaries allow for anterior-posterior movement

As described in 1.2, interframe movement is a large source of error.

The previous pipeline computes a single mask using the image taken at 410nm. This mask is then applied to both the 410nm and 470nm images. Measurements are taken of the masked image. Thus, if the animal pumps, measurement might start in the gut or halfway through the posterior bulb, depending on if the animal contracted during the first or second frame. If the animal contracts during the first frame and extends in the second, the mask will be too "short" and measurement in the second frame will start in the middle of the posterior bulb. If the animal is extended in the first frame and contracts in the second, the mask will be too "long" and measurement in the second frame will start in the gut.

The new approach is to create channel-specific masks for the purposes of drawing midlines. This allows the measurement boundaries to change on a frame-by-frame basis. That is, measurements always start at the posterior bulb and end at the tip.

2.3 Midlines

2.3.1 A transmitted light image helps to anchor the midlines

The previous centerline estimation algorithm takes as input an image of the pharynx aligned horizontally along its anterior posterior axis and works as follows (depicted

in figure 2.3).

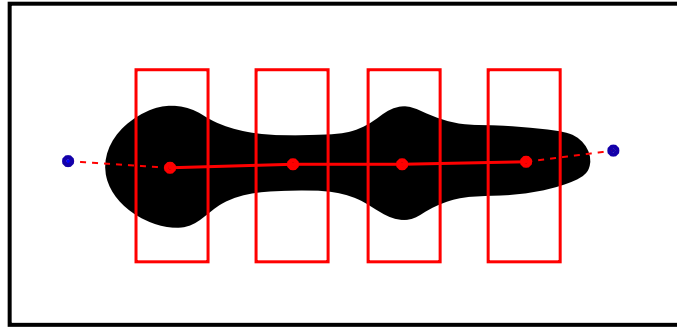


FIGURE 2.3: Cartoon representation of the previous centerline estimation algorithm.

Boxes are drawn at specific static coordinates. The centroid of each shape is calculated (red points). Lines (solid) connect these points. The y-coordinates of the terminating points (blue) is determined via the point-slope method $y = mx + b$ where m is the inverse of the slope of the neighboring line, x is a fixed constant and b is the y-coordinate of the neighboring point.

One problem

The current centerline estimation algorithm is unstable around the posterior bulb. These instabilities must be manually corrected. Fundamentally, this problem arises because the

2.3.2 Dorsal-ventral movement of the tip is a problem

We saw in 2.2 a strategy to combat the major mode of inter-frame movement, contractions of the posterior bulb. However, there is another less common mode: dorsal-ventral movement of the tip.

Again, frame-specific measurements are key to addressing this problem. Instead of using a single midline derived from the first frame, we calculate the midline independently in each frame. This frame-specific midline is then used to take profile measurements.

2.4 Channel Registration picks up the slack

The frame-specific midline approach discussed in 2.3.2 introduces problems of its own. Specifically, the length of the measurement vector may be stretched nonlinearly due to differences in the arc length of each midline. That is, some sections of the intensity profile measured under these lines might be stretched while others are compressed. To approach these nonlinear stretches and compressions, we utilized a functionalized version of the dynamic time warping algorithm.

explanation of fda registration

Chapter 3

Results

3.1 Definition of Error

To assess the degree to which changes to the analysis pipeline affect the quality of measurement, a definition of error must first be decided upon. Error is defined to be a function over pharynx space which is the difference between the intensity measured in one frame and another. The difference is divided by the average intensity of the two frames

$$\epsilon(p) = \frac{I_{410_1}(p) - I_{410_2}(p)}{\frac{I_{410_1}(p) + I_{410_2}(p)}{2}}$$

By examining differences of intensities emitted during exposure to only 410nm, we are not affected by actual redox patterning.

3.2 Collection of test data

A large number of technical replicates were collected. A single animal was imaged 57 times in pairs of two images both at 410nm.

describe conditions of image collection

It is possible that the first excitation of 410nm causes an endogenous response which would affect the fluorescence upon secondary exposure. A paired-sample t-test indicates no significant difference in the average intensity of the second image as compared to the first (p=0.41).

3.3 A Partially Synthetic Dataset Increases Statistical Power

Instead of comparing pairs of measurements taken back-to-back, we can compare all possible pairs. Given n images, we generate $\binom{n}{2} = \frac{n!}{2!(n-2)!}$ pairs. This is reasonable if we do not see a change in intensity over time.

make sure this relationship is real

3.4 Reductions in Manual Intervention

show figures comparing % requiring manual intervention for segmentation and for midlines

3.5 Channel-Specific Masks and Midlines Reduce Error

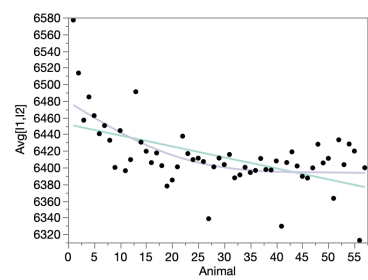


FIGURE 3.1: The average intensity over time in technical replicates

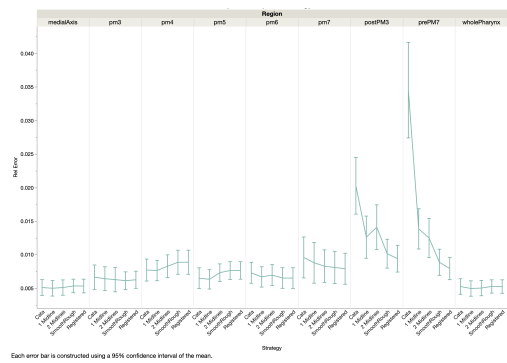


FIGURE 3.2: Relative error

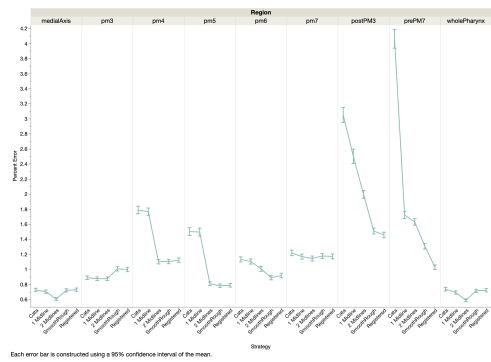


FIGURE 3.3

Chapter 4

Discussion

4.1 Future Directions